PAPER *Special Section on Radio Access Techniques for 3G Evolution*

RLS Channel Estimation with Adaptive Forgetting Factor for DS-CDMA Frequency-Domain Equalization

Yohei KOJIMA[†a)], **Hiromichi TOMEBA**[†], ***Student Members***, **Kazuaki TAKEDA**[†], ***Member***, ***and*** **Fumiyuki ADACHI**[†], ***Fellow***

SUMMARY Frequency-domain equalization (FDE) based on the minimum mean square error (MMSE) criterion can increase the downlink bit error rate (BER) performance of DS-CDMA beyond that possible with conventional rake combining in a frequency-selective fading channel. FDE requires accurate channel estimation. Recently, we proposed a pilot-assisted channel estimation (CE) based on the MMSE criterion. Using MMSE-CE, the channel estimation accuracy is almost insensitive to the pilot chip sequence, and a good BER performance is achieved. In this paper, we propose a channel estimation scheme using one-tap recursive least square (RLS) algorithm, where the forgetting factor is adapted to the changing channel condition by the least mean square (LMS) algorithm, for DS-CDMA with FDE. We evaluate the BER performance using RLS-CE with adaptive forgetting factor in a frequency-selective fast Rayleigh fading channel by computer simulation.

key words: *DS-CDMA, frequency-domain equalization, channel estimation, RLS algorithm*

1. Introduction

The 4th generation (4G) mobile communication systems [1] which provide broadband wireless services of e.g. 100 Mbps to 1 Gbps are expected around 2015. In the present 3rd generation (3G) systems, direct sequence-code division multiple access (DS-CDMA) is adopted as the wireless access technique [2]. However, since the broadband wireless channel is severely frequency-selective, the bit error rate (BER) performance of DS-CDMA with rake combining significantly degrades. The use of frequency-domain equalization (FDE) based on the minimum mean square error (MMSE) criterion can provide a better BER performance of DS-CDMA than the rake combining [3], [4].

FDE requires accurate estimation of the channel transfer function. Pilot-assisted channel estimation (CE) can be used. Time-domain pilot-assisted CE was proposed for single-carrier transmission in [5]. After the channel impulse response is estimated according to the least-sum-of-squared-error (LSSE) criterion, the channel transfer function is obtained by applying fast Fourier transform (FFT). Frequency-domain pilot-assisted CE was proposed in [6], [7]. The received pilot signal is transformed into the frequency-domain pilot signal and then the pilot modulation is removed using zero forcing (ZF) or least square (LS) technique. As the pilot signal, the Chu sequence [8] that has the constant amplitude in both time- and frequency-domain is used. However, the number of Chu sequences is limited. For example, it is only 128 for the case of 256-bit period [8].

PN sequences can be used for the pilot. Using a partial sequence taken from a long PN sequence, a very large number of pilots can be generated. However, since the frequency spectrum of the partial PN sequence is not constant, the use of ZF-CE produces noise enhancement [9]. The noise enhancement can be mitigated by the minimum mean square error channel estimation (MMSE-CE) [9]. Using MMSE-CE, the channel estimation accuracy is made almost insensitive to the pilot chip sequence. Recently, we proposed a 2-step maximum likelihood channel estimation (MLCE) to further improve the estimation accuracy [10]. However, the 2-step MLCE has the tracking ability problem in a fast fading environment since it assumes a block fading in which the channel gains stay constant over a frame. Channel estimation using recursive least square (RLS) algorithm was proposed to track the time-varying channels [11]. In [11], RLS algorithm and the superimposed training sequences are applied for channel estimation in orthogonal frequency division multiplexing (OFDM). However, the forgetting factor of RLS algorithm was not adapted in [11] and needs to be set according to the channel condition.

In this paper, we propose a channel estimation scheme using one-tap RLS algorithm, where the forgetting factor is adapted to the changing channel condition by the least mean square (LMS) algorithm, for DS-CDMA with FDE. We evaluate, by computer simulation, the BER performance of DS-CDMA using RLS-CE with adaptive forgetting factor in a frequency-selective fast Rayleigh fading channel. The achievable BER performance is compared with those using 2-step MLCE and using MMSE-CE with 1st order interpolation.

2. Transmission System Model

2.1 Overall Transmission System Model

The transmission system model for multicode DS-CDMA with FDE is illustrated in Fig. 1. Throughout the paper, the chip-spaced discrete-time signal representation is used. At the transmitter, a binary data sequence is transformed into data-modulated symbol sequence and then converted to U parallel streams by serial-to-parallel (S/P) conversion. Then,

Manuscript received August 25, 2008.

Manuscript revised December 25, 2008.

[†]The authors are with the Department of Electrical and Communication Engineering, Graduate School of Engineering, Tohoku University, Sendai-shi, 980-8579 Japan.

a) E-mail: kojima@mobile.ecei.tohoku.ac.jp

DOI: 10.1587/transcom.E92.B.1457

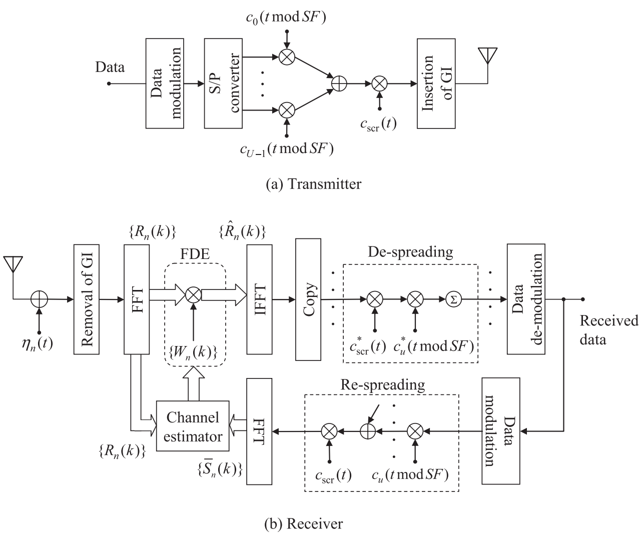

Fig. 1 Transmitter/receiver structure for DS-CDMA with FDE.

each parallel stream is divided into a sequence of blocks of N_c/SF symbols each, where N_c and SF denote the size of the chip-block and the spreading factor, respectively. The mth data symbol of the nth chip-block ($n = 0 \sim N-1$) in the uth stream is represented by $d_{n,u}(m)$, $m = 0 \sim N_c/SF-1$. $d_{n,u}(m)$ is spread by multiplying it with an orthogonal spreading sequence $\{c_u(t); t = 0 \sim SF-1\}$. The resultant U chip-blocks of N_c chips each are added and further multiplied by a common scramble sequence $\{c_{scr}(t); t = \ldots, 1, 0, 1, \ldots\}$ to make the resultant multicode DS-CDMA chip-block like white-noise. The last N_g chips of each N_c chip-block is copied as a cyclic prefix and inserted into the guard interval (GI) placed at the beginning of each chip-block, as illustrated in Fig. 2. For channel estimation, one pilot chip-block is transmitted every $N-1$ data chip-blocks to constitute a frame of N chip-blocks, as shown in Fig. 3.

The GI-inserted chip-block is transmitted over a frequency-selective fading channel and is received at a receiver. After removal of the GI, the received chip-block is decomposed by N_c-point FFT into N_c frequency components. The channel estimation using RLS-CE is performed as follows. The RLS-CE is carried out using the received pilot chip-block. Using the channel estimate, a series of MMSE-FDE, N_c-point inverse FFT (IFFT), de-spreading and data de-modulation is performed on the 1st data chip-block in the frame. Then, the chip-block replica is regenerated and the RLS-CE is carried out using the chip-block replica as a pilot. The forgetting factor used in the RLS algorithm is updated using the LMS algorithm (see Sect. 3). This is repeated until the reception of the last data chip-block in the frame.

2.2 Signal Representation

The nth chip-block $\{\tilde{s}_n(t); t = 0 \sim N_c-1\}$ can be expressed, using the equivalent lowpass representation, as

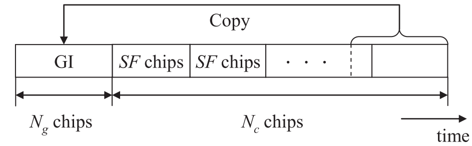

Fig. 2 Chip-block structure.

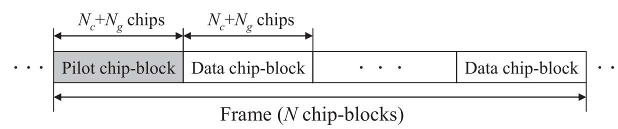

Fig. 3 Frame structure.

$$\tilde{s}_n(t) = \sqrt{2P} s_n(t) \tag{1}$$

with

$$s_n(t) = \left\{ \sum_{u=0}^{U-1} d_{n,u}\left(\left\lfloor \frac{t}{SF} \right\rfloor \right) c_u(t \bmod SF) \right\} c_{scr}(t), \tag{2}$$

where P is the transmit power and $\lfloor x \rfloor$ represents the largest integer smaller than or equal to x. After inserting the GI of N_g chips, the nth chip-block is transmitted. The propagation channel is assumed to be a frequency-selective fading channel having chip-spaced L discrete paths, each subjected to independent fading. The channel impulse response $h_n(\tau)$ can be expressed as

$$h_n(\tau) = \sum_{l=0}^{L-1} h_{n,l}\delta(\tau - \tau_l), \tag{3}$$

where $h_{n,l}$ and τ_l are the complex-valued path gain and time delay of the lth path ($l = 0 \sim L-1$), respectively, with $\sum_{l=0}^{L-1} \mathrm{E}[|h_{n,l}|^2] = 1$ (E[.] denotes the ensemble average operation). In this paper, we assume that the maximum time delay difference $\tau_{L-1} - \tau_0$ of the channel is shorter than the GI length. We assume that the path gains stay constant over one chip-block but change block by block.

The nth received chip-block $\{r_n(t); t = 0 \sim N_c-1\}$ can be expressed as

$$r_n(t) = \sum_{l=0}^{L-1} h_{n,l}\tilde{s}_n(t - \tau_l) + \eta_n(t), \tag{4}$$

where $\eta_n(t)$ is a zero-mean complex Gaussian process with variance $2N_0/T_c$ with T_c and N_0 being respectively the chip duration and the single-sided power spectrum density of the additive white Gaussian noise (AWGN).

2.3 MMSE-FDE

After the removal of the GI, the received chip-block is decomposed by an N_c-point FFT into N_c frequency components. The kth frequency component of the nth chip-block ($n = 0 \sim N-1$) can be written as

$$\begin{aligned}R_n(k) &= \sum_{t=0}^{N_c-1} r_n(t)\exp\left(-j2\pi k\frac{t}{N_c}\right)\\ &= H_n(k)S_n(k) + \Pi_n(k),\end{aligned} \tag{5}$$

where $H_n(k)$ is the channel gain, $S_n(k)$ is the signal component, and $\Pi_n(k)$ is the noise due to zero-mean AWGN. They are given by

$$\begin{cases} S_n(k) = \sum_{t=0}^{N_c-1} s_n(t)\exp\left(-j2\pi k\frac{t}{N_c}\right)\\ H_n(k) = \sqrt{2P}\sum_{l=0}^{L-1} h_{n,l}\exp\left(-j2\pi k\frac{\tau_l}{N_c}\right)\\ \Pi_n(k) = \sum_{t=0}^{N_c-1} \eta_n(t)\exp\left(-j2\pi k\frac{t}{N_c}\right). \end{cases} \tag{6}$$

One-tap MMSE-FDE is carried out as

$$\hat{R}_n(k) = W_n(k)R_n(k), \tag{7}$$

where $W_n(k)$ is the MMSE-FDE weight and is given by [3], [4]

$$W_n(k) = \frac{H_n^*(k)}{UN_c|H_n(k)|^2 + 2\sigma^2} \tag{8}$$

with $2\sigma^2$ ($= 2N_0N_c/T_c$) being the variance of $\Pi_n(k)$ and $*$ denoting the complex conjugate operation. $H_n(k)$ and σ^2 are unknown to the receiver and need to be estimated. In this paper, $H_n(k)$ is estimated by RLS-CE. σ^2 can be estimated according to [9].

N_c-point IFFT is applied to transform the frequency-domain signal $\{\hat{R}_n(k); k = 0 \sim N_c-1\}$ into the time-domain chip-block $\{\hat{r}_n(t); t = 0\sim N_c-1\}$ as

$$\hat{r}_n(t) = \frac{1}{N_c}\sum_{k=0}^{N_c-1}\hat{R}_n(k)\exp\left(j2\pi t\frac{k}{N_c}\right). \tag{9}$$

Finally, de-spreading is carried out on $\{\hat{r}_n(t)\}$, giving

$$\hat{d}_{n,u}(m) = \frac{1}{SF}\sum_{t=mSF}^{(m+1)SF-1}\hat{r}_n(t)c_u^*(t \bmod SF)c_{\mathrm{scr}}^*(t), \tag{10}$$

which is the decision variable for data de-modulation on $\hat{d}_{n,u}(m)$.

3. RLS Channel Estimation Using Adaptive Forgetting Factor

The channel estimate of $H_n(k)$ is denoted by $\tilde{H}_n(k)$. In Sect. 3.1, we present the one-tap RLS algorithm for the channel estimation. Then, the forgetting factor adaptation is described in Sect. 3.2. The chip-block replica is generated to be used as a pilot in the channel estimation for MMSE-FDE of the next chip-block. The noise reduction in the channel estimate is done by applying the delay-time domain windowing technique [12], [13]. These are presented in Sect. 3.3. In Sect. 3.4, the computational complexity of the proposed RLS-CE is compared with 2-step MLCE [10], MMSE-CE with decision-feedback [9], and MMSE-CE with 1st order interpolation.

3.1 One-Tap RLS Algorithm

One-tap RLS algorithm is illustrated in Fig. 4. We use the following cost function for the RLS algorithm [14]:

$$\varepsilon_n(k) = \sum_{i=1}^{n}\lambda^{n-i}|e_i(k)|^2, \tag{11}$$

where $e_i(k)$ is given by

$$e_i(k) = R_i(k) - \tilde{H}_n(k)S_i(k), \tag{12}$$

where λ ($0 < \lambda \leq 1$) is the forgetting factor. The channel estimate $\tilde{H}_n(k)$ is the one that minimizes $\varepsilon_n(k)$. Solving $\partial\varepsilon_n(k)/\partial\tilde{H}_n(k) = 0$ gives

$$\tilde{H}_n(k) = Z_n(k)/\Phi_n(k), \tag{13}$$

where $Z_n(k)$ and $\Phi_n(k)$ are respectively given by

$$\begin{cases} Z_n(k) = \sum_{i=1}^{n}\lambda^{n-i}R_i(k)S_i^*(k)\\ \Phi_n(k) = \sum_{i=1}^{n}\lambda^{n-i}|S_i(k)|^2. \end{cases} \tag{14}$$

To update $Z_n(k)$ and $\Phi_n(k)$ recursively, they are rewritten as

$$\begin{cases} Z_n(k) = \lambda Z_{n-1}(k) + R_n(k)S_n^*(k)\\ \Phi_n(k) = \lambda\Phi_{n-1}(k) + |S_n(k)|^2. \end{cases} \tag{15}$$

Substituting Eq. (15) into Eq. (13) gives the following update equation based on the RLS algorithm:

$$\tilde{H}_n(k) = \tilde{H}_{n-1}(k) + G_n(k)\xi_n(k), \tag{16}$$

where

$$\begin{cases} G_n(k) = S_n^*(t)/\Phi_n(k)\\ \xi_n(k) = R_n(k) - \tilde{H}_{n-1}(k)S_n(k). \end{cases} \tag{17}$$

The optimum forgetting factor λ changes according to the change in the channel statistical property (i.e., fading rate and fading type). In this paper, assuming that channel statistical property does not change rapidly, λ is adapted by the LMS algorithm [14].

3.2 Adaptive Algorithm of Forgetting Factor λ

The following cost function is used:

$$J_n(k) = \frac{1}{2}\mathrm{E}\left[|\xi_n(k)|^2\right]. \tag{18}$$

Finding λ that minimizes Eq. (18) corresponds to the steepest descent method as

$$\lambda_n(k) = \lambda_{n-1}(k) + \mu\left(-\nabla\lambda_n(k)\right), \tag{19}$$

where μ is the step size and the gradient vector $\nabla\lambda_n(k)$ is the differentiation of the cost function $J_n(k)$ with respect to λ. $\nabla\lambda_n(k)$ is given as

$$\nabla\lambda_n(k) = \frac{\partial J_n(k)}{\partial\lambda} = -\mathrm{Re}[\mathrm{E}[\Psi_{n-1}(k)S_n(k)\xi_n^*(k)]], \tag{20}$$

where

$$\Psi_n(k) = \frac{\partial\tilde{H}_n(k)}{\partial\lambda}. \tag{21}$$

Substituting Eqs. (16) and (18) into (21) gives

$$\Psi_n(k) = (1 - G_n(k)S_n(k))\,\Psi_{n-1}(k) + \frac{\partial\Phi_n^{-1}(k)}{\partial\lambda}S_n^*(k)\xi_n(k). \tag{22}$$

Differentiation of inverse of Eq. (15) with respect to λ gives the updating equation for $\partial\Phi_n^{-1}(k)/\partial\lambda$ as

$$\frac{\partial\Phi_n^{-1}(k)}{\partial\lambda} = \lambda^{-1}\left\{(1 - G_n(k)S_n(k))^2\frac{\partial\Phi_{n-1}^{-1}(k)}{\partial\lambda} + |G_n(k)|^2 + \Phi_n^{-1}(k)\right\}. \tag{23}$$

The above mentioned steepest descent method requires the gradient vector $\nabla\lambda_n(k)$ at each iteration n. However, $\nabla\lambda_n(k)$ is unknown and must be estimated using the available data. The instantaneous estimate of $\nabla\lambda_n(k)$ on the basis of Eq. (20) is

$$\hat{\nabla}\lambda_n(k) = -\mathrm{Re}[\Psi_{n-1}(k)S_n(k)\xi_n^*(k)]. \tag{24}$$

Replacing $\nabla\lambda_n(k)$ in Eq. (19) by Eq. (24), we obtain the following LMS algorithm for updating the forgetting factor:

$$\lambda_n(k) = \lambda_{n-1}(k) + \mu\mathrm{Re}[\Psi_{n-1}(k)S_n(k)\xi_n^*(k)]. \tag{25}$$

The forgetting factor $\lambda_n(k)$ depends on statistical characteristics of the fading channel. Statistical characteristics are identical for all frequencies. Therefore, in this paper, $\lambda_n = (1/N_c)\sum_{k=0}^{N_c-1}\lambda_n(k)$ is used to suppress the noise.

The proposed RLS-CE requires the knowledge of the transmitted chip-block $\{S_n(k); k = 0\sim N_c-1\}$, $n \geq 1$. However, since $\{S_n(k); k = 0\sim N_c-1\}$ is unknown at the receiver, the transmitted chip-block replica $\{\hat{S}_n(k); k = 0 \sim N_c-1\}$ needs to be generated by the decision-feedback. This is done as follows. First, MMSE-FDE (Eqs. (7) and (8)) is carried out using the channel estimate for the $(n-1)$th chip-block. After performing a series of MMSE-FDE, N_c-point IFFT, de-spreading and data de-modulation on the nth chip-block, the tentatively detected symbol sequence $\{\bar{d}_{n,u}(m); m = 0 \sim N_c/SF-1\}$, $u = 0 \sim U-1$, is spread to generate the transmitted chip-block replica $\{\bar{s}_n(t); t = 0\sim N_c-1\}$:

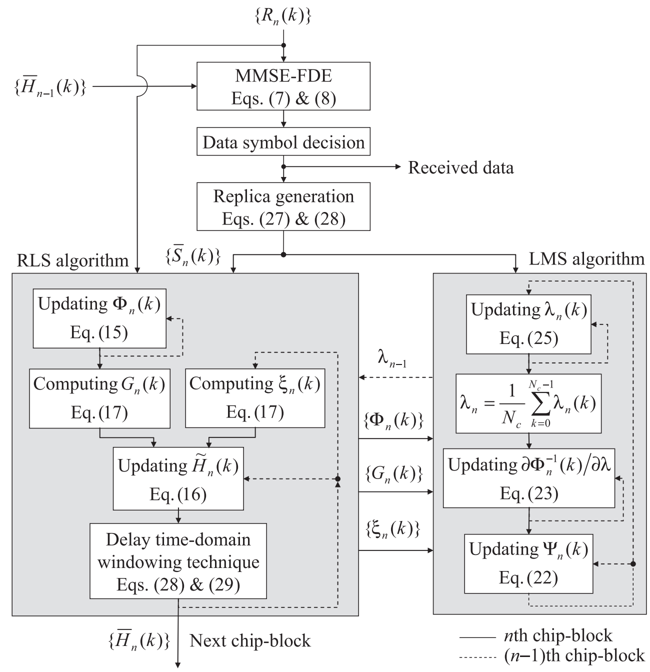

Fig. 4 One-tap RLS algorithm using adaptive forgetting factor.

$$\bar{s}_n(t) = \left\{\sum_{u=0}^{U-1}\bar{d}_{n,u}\left(\left\lfloor\frac{t}{SF}\right\rfloor\right)c_u(t \bmod SF)\right\}c_{\mathrm{scr}}(t). \tag{26}$$

The chip-block replica is transformed by an N_c-point FFT into N_c frequency components $\{\bar{S}_n(k); k = 0 \sim N_c - 1\}$. The kth frequency component $\bar{S}_n(k)$ of the transmitted chip-block replica is obtained as

$$\bar{S}_n(k) = \sum_{t=0}^{N_c-1}\bar{s}_n(t)\exp\left(-j2\pi k\frac{t}{N_c}\right). \tag{27}$$

Using $\{\bar{S}_n(k); k = 0\sim N_c-1\}$ instead of $\{S_n(k); k = 0\sim N_c-1\}$, the channel estimate $\{\tilde{H}_n(k); k = 0\sim N_c - 1\}$ for the nth chip-block is obtained by RLS algorithm (Eqs. (16) and (17)). The forgetting factor λ_n is updated by LMS algorithm (Eqs. (22), (23) and (25)).

The flowchart of the above-mentioned one-tap RLS algorithm using adaptive forgetting factor is illustrated in Fig. 4.

3.3 Further Improvement by Delay Time-Domain Windowing Technique

The instantaneous channel estimate $\{\tilde{H}_n(k); k = 0 \sim N_c-1\}$ obtained by RLS-CE is perturbed by the noise due to the AWGN. In this paper, the delay time-domain windowing technique [12], [13] is introduced to reduce the noise. The instantaneous channel estimate $\{\tilde{H}_n(k); k = 0 \sim N_c-1\}$ is transformed by N_c-point IFFT into the instantaneous channel impulse response $\{\tilde{h}_n(\tau); \tau = 0\sim N_c-1\}$ as

$$\tilde{h}_n(\tau) = \frac{1}{N_c}\sum_{k=0}^{N_c-1}\tilde{H}_n(k)\exp\left(j2\pi\tau\frac{k}{N_c}\right). \tag{28}$$

The actual channel impulse response is present only within the GI length, while the noise is spread over an entire delay-time range. Replacing $\tilde{h}_n(\tau)$ with zero's for $N_g \le \tau \le N_c-1$ and applying N_c-point FFT, the improved channel estimate $\{\bar{H}_n(k); k = 0\sim N_c-1\}$ is obtained as

$$\bar{H}_n(k) = \sum_{\tau=0}^{N_g-1} \tilde{h}_n(\tau)\exp\left(-j2\pi k\frac{\tau}{N_c}\right). \tag{29}$$

The MMSE-FDE weight of the $(n+1)$th chip-block is computed using Eq. (8) by replacing $H_n(k)$ by $\bar{H}_n(k)$. The channel estimate of the $(n+1)$th chip-block is updated using $\bar{H}_n(k)$.

3.4 Complexity Comparison

The computational complexity of the proposed RLS-CE is compared with 2-step MLCE [10], MMSE-CE with decision-feedback [9], and MMSE-CE with 1st order interpolation in terms of the number of complex multiplication operations (CMOs) per frame. Noting that N_c-point FFT (and also IFFT) operation requires $(N_c/2)\log_2 N_c$ CMOs, Table 1 compares four channel estimation schemes. For $SF = 16$, $U = 16$, $N_c = 256$, and $N = 16$, it can be shown that the complexity of RLS-CE is approximately 1.2 times higher than MMSE-CE with decision-feedback and is approximately 1.9 times higher than MMSE-CE with 1st order interpolation. However, the complexity of RLS-CE is approximately 0.8 times that of 2-step MLCE.

Table 1 CMOs of four channel estimation schemes.

No. of CMOs per frame	RLS-CE	2-step MLCE [10]
RLS-CE	$N(16N_c+1)$	—
MMSE-CE	—	$3N_c$
MLCE	—	$(N+1)N_c$
Delay time-domain windowing	$NN_c\log_2 N_c$	$2N_c\log_2 N_c$
FDE & IFFT & de-spreading	$(N-1)\{3N_c$ $+(N_c/2)\log_2 N_c$ $+U(N_c/SF)(2SF+1)\}$	$2(N-1)\{3N_c$ $+(N_c/2)\log_2 N_c$ $+U(N_c/SF)(2SF+1)\}$
Data chip-block replica generation	$(N-1)\{N_c(U+1)$ $+(N_c/2)\log_2 N_c\}$	$(N-1)\{N_c(U+1)$ $+(N_c/2)\log_2 N_c\}$

No. of CMOs per frame	MMSE-CE with decision-feedback [9]	MMSE-CE with 1st order interpolation
MMSE-CE	$3NN_c$	$6N_c$
1st order interpolation	—	$8N_c$
Delay time-domain windowing	$NN_c\log_2 N_c$	$2N_c\log_2 N_c$
1st order filtering	$2(N-1)N_c$	—
FDE & IFFT & de-spreading	$(N-1)\{3N_c$ $+(N_c/2)\log_2 N_c$ $+U(N_c/SF)(2SF+1)\}$	$(N-1)\{3N_c$ $+(N_c/2)\log_2 N_c$ $+U(N_c/SF)(2SF+1)\}$
Data chip-block replica generation	$(N-1)\{N_c(U+1)$ $+(N_c/2)\log_2 N_c\}$	—

4. Computer Simulation

The simulation condition is shown in Table 2. We assume 16QAM data modulation, an FFT block size of $N_c = 256$ chips and a GI of $N_g = 32$ chips. One pilot chip-block is transmitted every 15 data chip-blocks (i.e., $N = 16$). We assume the spreading factor $SF = 16$ and an $L=16$-path frequency-selective Rayleigh fading channel having uniform power delay profile. The initial value of λ is set to $\lambda_{-1} = 0.7$.

Figurs 5(a) and 5(b) show the convergence performance of forgetting factor λ and that of block-average BER, respectively, with the normalized Doppler frequency f_DT (where T $(=(N_c+N_g)T_c)$ is the chip-block length) as a parameter for the full code-multiplexing case ($U = SF = 16$) at $E_b/N_0 = 24$ dB. As seen from Fig. 5(a), the convergence rate of λ tends to become slower when smaller value of μ is used for $f_DT = 1\times10^{-4}$, 1×10^{-3} and 5×10^{-3}. However, it can be seen from Fig. 5(b) that the convergence rate of the block-average BER is similar even if which value of $\mu = 5\times10^{-6}$, 1×10^{-5} or 1×10^{-4} is used when $f_DT = 1\times10^{-4}$ and 1×10^{-3}. On the other hand, when $f_DT = 5\times10^{-3}$ (fast fading), the convergence rate of the block-average BER is different for a different value of μ. Because of limitation in the tracking capability against fast fading, the block-average BER periodically varies at the pilot block insertion cycle (or frame period) even if which value of μ is used. However, it can be seen that the use of $\mu = 5\times10^{-6}$ provides the minimum BER. Below, $\mu = 5\times10^{-6}$ is used.

Figure 6 shows the impact of fading rate on the achievable BER as a function of the normalized Doppler frequency f_DT at $E_b/N_0 = 24$ dB for the full code-multiplexing case ($U = SF = 16$). It is seen from Fig. 6 that the forgetting

Table 2 Simulation condition.

Transmitter	Data modulation	16QAM
	FFT block size	$N_c = 256$
	Guard interval length	$N_g = 32$
	Spreading sequence	Product of Walsh sequence and PN sequence
	Spreading factor	$SF = 16$
	Code multiplexing order	$U = 1, 16$
	Pilot chip sequence	PN sequence
	No. of chip-blocks/frame	$N = 16$
Channel	Fading	Frequency-selective block Rayleigh
	Power delay profile	$L=16$-path uniform power delay profile
Receiver	Frequency-domain equalization	MMSE
	Channel estimation	RLS-CE ($\mu = 5\times10^{-6}$)

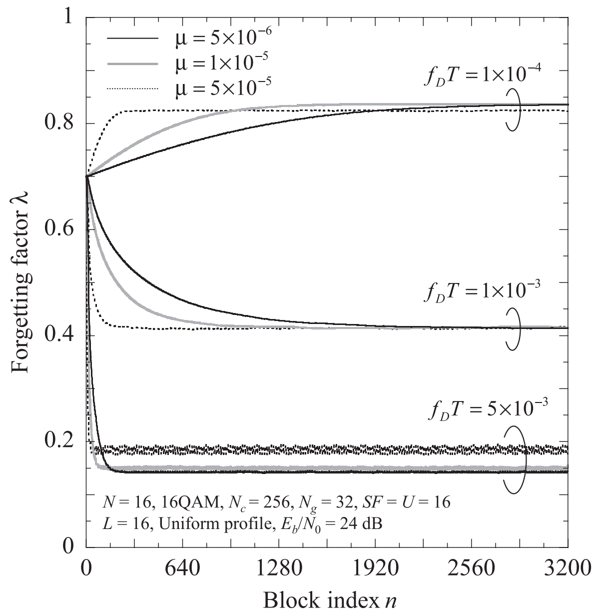

(a) Forgetting factor λ.

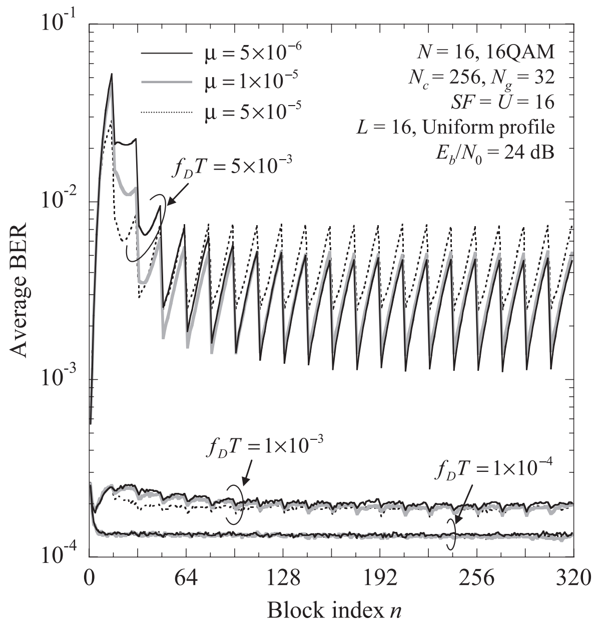

(b) Block-average BER.

Fig. 5 Convergence performance.

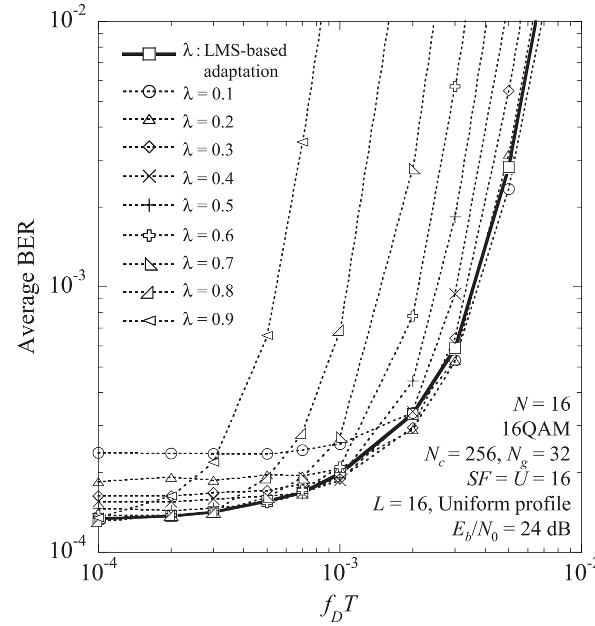

Fig. 6 Impact of fading rate.

factor λ can be optimally adjusted by LMS algorithm over all f_DT's.

The simulated BER performance of multicode DS-CDMA using RLS-CE is plotted in Fig. 7 for $U = 1$ and 16 as a function of the average received bit energy-to-AWGN noise power spectrum density ratio E_b/N_0 ($= 0.25(P \cdot SF \cdot T_c/N_0)(1 + N_g/N_c)N/(N-1)$). The BER performances using 2-step MLCE, pilot-assisted MMSE-CE with decision-feedback, MMSE-CE with 1st order interpolation and ideal CE are also plotted for comparison.

First, the $U = 1$ case is discussed. It is seen from Fig. 7 that RLS-CE provides a better BER performance than MMSE-CE with decision-feedback and MMSE-CE with 1st order interpolation. The E_b/N_0 loss from the ideal CE case for BER $= 10^{-4}$ is about 0.8 (1) dB for MMSE-CE with decision-feedback when $f_DT = 5 \times 10^{-4}$ (10^{-3}), but about 1.3 dB for MMSE-CE with 1st order interpolation when $f_DT = 5 \times 10^{-4}$ and 10^{-3}. The E_b/N_0 loss includes a pilot insertion loss of 0.28 dB. RLS-CE gives the E_b/N_0 loss of about 0.4 (0.5) dB which is the same as 2-step MLCE when $f_DT = 5 \times 10^{-4}$ (10^{-3}).

Next, the $U = 16$ case is discussed. When $f_DT = 5 \times 10^{-4}$ (see Fig. 7(a)), RLS-CE provides a better BER performance than 2-step MLCE, MMSE-CE with decision-feedback and MMSE-CE with 1st order interpolation. When $f_DT = 10^{-3}$ (see Fig. 7(b)), RLS-CE provides a better BER performance than 2-step MLCE and MMSE-CE with decision-feedback. It provides a same BER performance as MMSE-CE with 1st order interpolation.

Figure 8 shows the impact of fading rate on the achievable BER at $E_b/N_0 = 24$ dB as a function of the normalized Doppler frequency f_DT for the full code-multiplexing case ($U = SF = 16$). For comparison, the BER performance using 2-step MLCE, pilot-assisted MMSE-CE with decision-feedback and MMSE-CE with 1st order interpolation are also plotted. It is seen from Fig. 8 that RLS-CE always provides a better BER performance than 2-step MLCE and MMSE-CE with decision-feedback. However, RLS-CE is inferior to MMSE-CE with 1st order interpolation if $f_DT \geq 10^{-3}$. As an example, assume a CDMA system of chip-rate $1/T_c = 100$ Mcps (bandwidth of 100 MHz) and $SF = 16$ using 3.5 GHz carrier frequency (the global use of 3.4 ~ 3.6 GHz has been allocated for IMT advanced systems in Nov. 2007 by ITU-R [15]), f_DT becomes 10^{-3} when the moving speed reaches $v = 107$ km/h. Therefore, RLS-CE

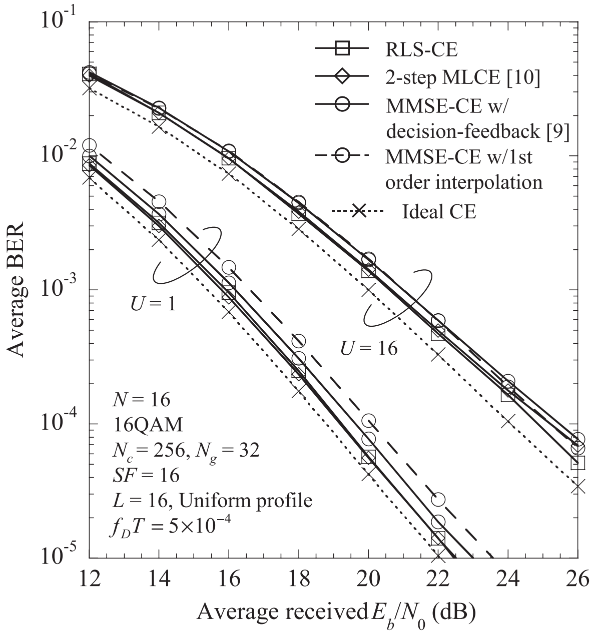

(a) $f_D T = 5\times10^{-4}$

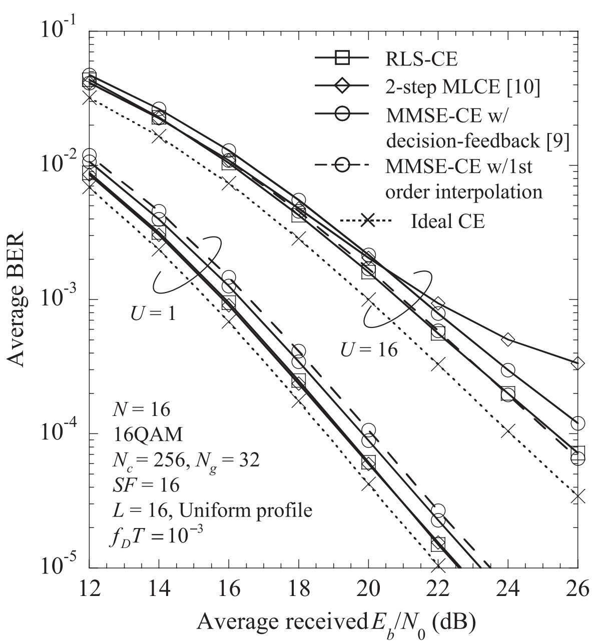

(b) $f_D T = 10^{-3}$

Fig. 7 BER performance comparison.

can be superior to MMSE-CE with 1st order interpolation if $v \leq 107$ km/h. If the terminal speed is above this speed, then MMSE-CE with 1st order interpolation should be used.

5. Conclusions

In this paper, we proposed a one-tap RLS-CE with adaptive forgetting factor for multicode DS-CDMA with FDE. It was shown by computer simulation that the proposed RLS-CE improves the BER performance compared to 2-step MLCE and pilot-assisted MMSE-CE with decision-feedback. RLS-CE with adaptive forgetting factor has a better tracking ability against the fading variation and provides a better BER performance than MMSE-CE with 1st order interpolation for the normalized Doppler frequency $f_D T \leq 10^{-3}$.

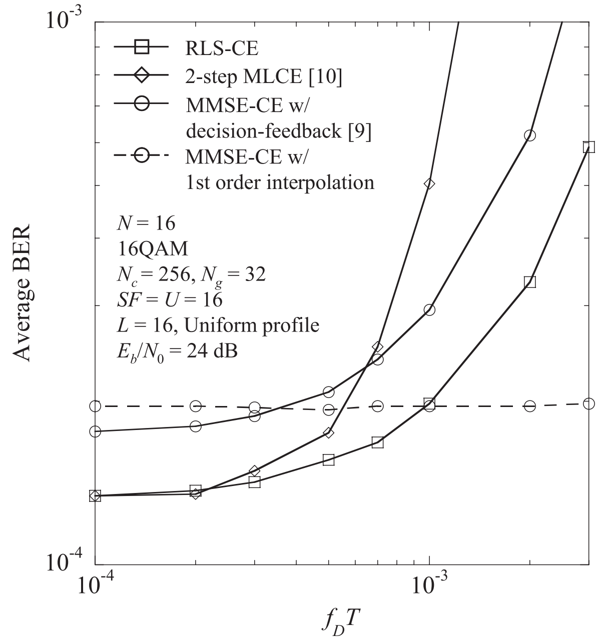

Fig. 8 Impact of fading rate.

References

[1] Y. Kim, B.J. Jeong, J. Chung, C.-S. Hwang, J.S. Ryu, K.-H. Kim, and Y.K. Kim, "Beyond 3G: Vision, requirements, and enabling technologies," IEEE Commun. Mag., vol.41, no.3, pp.120–124, March 2003.

[2] F. Adachi, M. Sawahashi, and H. Suda, "Wideband DS-CDMA for next generation mobile communications systems," IEEE Commun. Mag., vol.36, no.9, pp.56–69, Sept. 1998.

[3] F.W. Vook, T.A. Thomas, and K.L. Baum, "Cyclic-prefix CDMA with antenna diversity," Proc. IEEE 55th VTC2002-Spring, pp.1002–1006, Birmingham, Al, May 2002.

[4] F. Adachi, D. Garg, S. Takaoka, and K. Takeda, "Broadband CDMA techniques," IEEE Wireless Commun. Mag., vol.12, no.2, pp.8–18, April 2005.

[5] Q. Zhang and T. Le-Ngoc, "Channel-estimate-based frequency-domain equalization (CE-FDE) for broadband single-carrier transmission," Wireless Commun. Mob. Comput., vol.4, no.4, pp.449–461, June 2004.

[6] C.-T. Lam, D. Falconer, F. Danilo-Lemoine, and R. Dinis, "Channel estimation for SC-FDE systems using frequency domain multiplexed pilots," Proc. IEEE 64th Veh. Technol. Conf. (VTC2006-Fall), pp.1–5, Montreal, Canada, Sept. 2006.

[7] D. Falconer, S.L Ariyavisitakul, A. Benyamin-Seeyar, and B. Eidson, "Frequency domain equalization for single-carrier broadband wireless systems," IEEE Commun. Mag., vol.40, no.4, pp.58–66, April 2002.

[8] D.C. Chu, "Polyphase codes with good periodic correlation properties," IEEE Trans. Inf. Theory, vol.18, no.4, pp.531–532, July 1972.

[9] K. Takeda and F. Adachi, "Frequency-domain MMSE channel estimation for frequency-domain equalization of DS-CDMA signals," IEICE Trans. Commun., vol.E90-B, no.7, pp.1746–1753, July 2007.

[10] Y. Kojima, K. Takeda, and F. Adachi, "2-step maximum likelihood channel estimation for DS-CDMA with frequency-domain equalization," Proc. 4th IEEE VTS Asia Pacific Wireless Communications Symposium (APWCS2007), National Chiao Tung University, Hsinchu, Taiwan, Aug. 2007.
[11] J. Zhan, J. Wang, S. Liu, and J.-W. Chong, "Channel estimation for OFDM systems based on RLS and superimposed training sequences," IEEE Wireless Commun., Networking and Mobile Computing, 2007. WiCom 2007. International Conference, pp.37–40, Sept. 2007.
[12] J.-J. van de Beek, O. Edfors, M. Sandell, S.K. Wilson, and P.O. Borjesson, "On channel estimation in OFDM systems," Proc. IEEE 45th VTC1995-Spring, pp.815–819, Chicago, IL, July 1995.
[13] T. Fukuhara, H. Yuan, Y. Takeuchi, and H. Kobayashi, "A novel channel estimation method for OFDM transmission technique under fast time-variant fading channel," Proc. IEEE 57th VTC2003-Spring, pp.2343–2347, Jeju, Korea, April 2003.
[14] S. Haykin, Adaptive Filter Theory, Prentice-Hall, Englewood Cliffs, NJ,1991.
[15] Final Acts WRC-07, Geneva, Nov. 2007.

Appendix A: Derivation of Eq. (22)

Substituting Eq. (16) into Eq. (21) gives

$$\Psi_n(k) = \frac{\partial \tilde{H}_{n-1}(k)}{\partial \lambda} + \frac{\partial G_n(k)}{\partial \lambda}\xi_n(k) + G_n(k)\frac{\partial \xi_n(k)}{\partial \lambda}. \quad (\mathrm{A}\cdot 1)$$

By substituting Eq. (17) into Eq. (A·1), we have

$$\Psi_n(k) = (1 - G_n(k)S_n(k))\,\Psi_{n-1}(k) + \frac{\partial \Phi_n^{-1}(k)}{\partial \lambda} S_n^*(k)\xi_n(k). \quad (\mathrm{A}\cdot 2)$$

Appendix B: Derivation of Eq. (23)

$\Phi_n^{-1}(k)$ of Eq. (15) can be rewritten as

$$\Phi_n^{-1}(k) = \lambda^{-1}\Phi_{n-1}^{-1}(k) - \frac{\lambda^{-2}\left(\Phi_{n-1}^{-1}(k)\right)^2 |S_n(k)|^2}{1 + \lambda^{-1}\Phi_{n-1}^{-1}(k)\,|S_n(k)|^2}. \quad (\mathrm{A}\cdot 3)$$

$\partial \Phi_n^{-1}(k)/\partial \lambda$ is given by

$$\frac{\partial \Phi_n^{-1}(k)}{\partial \lambda} = -\lambda^{-2}\Phi_{n-1}^{-1}(k) + \lambda^{-1}\frac{\partial \Phi_{n-1}^{-1}(k)}{\partial \lambda} - \frac{\partial}{\partial \lambda}\left(\frac{\lambda^{-2}\left(\Phi_{n-1}^{-1}(k)\right)^2 |S_n(k)|^2}{1 + \lambda^{-1}\Phi_{n-1}^{-1}(k)\,|S_n(k)|^2}\right). \quad (\mathrm{A}\cdot 4)$$

The 3rd term for Eq. (A·4) can be rewritten as

$$\frac{\partial}{\partial \lambda}\left(\frac{\lambda^{-2}\left(\Phi_{n-1}^{-1}(k)\right)^2 |S_n(k)|^2}{1 + \lambda^{-1}\Phi_{n-1}^{-1}(k)\,|S_n(k)|^2}\right) = \lambda^{-1}\left\{\left(2G_n(k)S_n(k) - |G_n(k)|^2|S_n(k)|^2\right) \times \frac{\partial \Phi_{n-1}^{-1}(k)}{\partial \lambda} - |G_n(k)|^2 - \frac{\lambda^{-2}\left(\Phi_{n-1}^{-1}(k)\right)^2 |S_n(k)|^2}{1 + \lambda^{-1}\Phi_{n-1}^{-1}(k)\,|S_n(k)|^2}\right\}. \quad (\mathrm{A}\cdot 5)$$

Hence, we have

$$\frac{\partial \Phi_n^{-1}(k)}{\partial \lambda} = \lambda^{-1}\left\{(1 - G_n(k)S_n(k))^2\frac{\partial \Phi_{n-1}^{-1}(k)}{\partial \lambda} + |G_n(k)|^2 + \Phi_n^{-1}(k)\right\}. \quad (\mathrm{A}\cdot 6)$$

Yohei Kojima received his B.E. degree in communications engineering from Tohoku University, Sendai, Japan, in 2007. Currently he is a graduate student at the Department of Electrical and Communications Engineering, Tohoku University. His research interests include channel estimation and equalization for mobile communication systems.

Hiromichi Tomeba received his B.S., M.S., and Dr.Eng. degrees in communications engineering from Tohoku University, Sendai, Japan, in 2004, 2006, and 2008, respectively. Currently he is a postdoctoral fellow at the Department of Electrical and Communications Engineering, Graduate School of Engineering, Tohoku University. Since 2006, he has been a Japan Society for the Promotion of Science (JSPS) research fellow. His research interests include frequency-domain equalization and antenna diversity techniques for mobile communication systems. He was a recipient of the 2004 and 2005 IEICE RCS (Radio Communication Systems) Active Research Award.

Kazuaki Takeda received his B.E., M.S. and Dr.Eng. degrees in communications engineering from Tohoku University, Sendai, Japan, in 2003, 2004 and 2007 respectively. Currently he is a postdoctoral fellow at the Department of Electrical and Communications Engineering, Graduate School of Engineering, Tohoku University. Since 2005, he has been a Japan Society for the Promotion of Science (JSPS) research fellow. His research interests include equalization, interference cancellation, transmit/receive diversity, and multiple access techniques. He was a recipient of the 2003 IEICE RCS (Radio Communication Systems) Active Research Award and 2004 Inose Scientific Encouragement Prize.

Fumiyuki Adachi received the B.S. and Dr.Eng. degrees in electrical engineering from Tohoku University, Sendai, Japan, in 1973 and 1984, respectively. In April 1973, he joined the Electrical Communications Laboratories of Nippon Telegraph & Telephone Corporation (now NTT) and conducted various types of research related to digital cellular mobile communications. From July 1992 to December 1999, he was with NTT Mobile Communications Network, Inc. (now NTT DoCoMo, Inc.), where he led a research group on wideband/broadband CDMA wireless access for IMT-2000 and beyond. Since January 2000, he has been with Tohoku University, Sendai, Japan, where he is a Professor of Electrical and Communication Engineering at the Graduate School of Engineering. His research interests are in CDMA wireless access techniques, equalization, transmit/receive antenna diversity, MIMO, adaptive transmission, and channel coding, with particular application to broadband wireless communications systems. From October 1984 to September 1985, he was a United Kingdom SERC Visiting Research Fellow in the Department of Electrical Engineering and Electronics at Liverpool University. Dr. Adachi served as a Guest Editor of IEEE JSAC on Broadband Wireless Techniques, October 1999, Wideband CDMA I, August 2000, Wideband CDMA II, Jan. 2001, and Next Generation CDMA Technologies, Jan. 2006. He is an IEEE Fellow and was a co-recipient of the IEEE Vehicular Technology Transactions Best Paper of the Year Award 1980 and again 1990 and also a recipient of Avant Garde award 2000. He was a recipient of IEICE Achievement Award 2002 and a co-recipient of the IEICE Transactions Best Paper of the Year Award 1996 and again 1998. He was a recipient of Thomson Scientific Research Front Award 2004.